THE MEASUREMENT OF COMPRESSIBILITY OF FRACTURED ROCK

X.L. Zhao, Q. Ma and **J.-C. Roegiers**
School of Petroleum & Geological Engineering
The University of Oklahoma
Norman, OK 73019, USA

ABSTRACT

An attempt was made in this paper to develop experimental techniques to determine the compressibility of fractured rock. A model was written on the basis of continuum damage mechanics, using the concept of material deterioration induced by structural rearrangements as an indirect measure of the fractures characterized by a so-called damage tensor **D**. By using effective properties of fractured rock, the detailed information about fractures is no longer important and, therefore, the material can be treated as a continuum medium.

Two rocks, Berea sandstone and Cordoba Cream limestone, were tested in three separate directions. Compressional- and shear-wave velocities at various confining pressures were also measured, in addition to mechanical measurements. The initial changes in compressibility with pressure due to the closing of fractures are related to the damage tensor **D**.

INTRODUCTION

For the past decades, elasticity theory has been used in reservoir characterization to calculate the stresses and to predict fractures. However, such an approach to represent discontinuities is total inappropriate, because the nucleation and coalescence of pores, inclusions, and cracks have a profound effect on the strength and properties of a material. To describe and solve this problem, two common methods can be used (Janson, 1978): (*i*) linear elastic fracture mechanics (LEFM); and, (*ii*) continuum damage mechanics (CDM).

Griffith (1920) gave the first successful analysis of a fracture-dominant problem. His fracture energy theory was further extended by Irwin (1957). The well-known concepts of energy release rate $\mathcal{G}$ and stress intensity factor K have become the basis of fracture mechanics, a well-established branch of applied mechanics. Utilizing the principles of LEFM, the effective elastic moduli, the stability, and the strength of rock containing a random distribution of interacting cracks have been studied by several researchers, Brace (1965); Walsh (1965a,b,c&d); Salganik (1973, 1974); O'Connell and Budiansky (1974); Vavakin and Salganik (1975); Bruner (1976); and, Kemeny and Cook (1986) among them. The effective mechanical properties of fractured rock have been found to relate to the original properties, for example bulk modulus K (the inverse of compressibility), as:

$$\frac{\tilde{K}}{K} = \frac{1}{1 + k\chi} \tag{1}$$

where $\tilde{K}$ is the effective bulk modulus; k is a parameter related to the shape of the cracks and material's Poisson's ratio; and, χ is the crack density.

If one takes into account the effect of crack interaction, a self-consistent method should be used; therefore, the above equation becomes:

$$\frac{\tilde{K}}{K} = 1 - \tilde{k}\chi \tag{2}$$

where $\tilde{k}$ is a parameter related to the shape of the cracks and the effective Poisson's ratio. Unfortunately, a serious limitation to the practical use of such models lies in the fact that the crack dimensions and the number of cracks are very difficult to be estimated.

The concept of continuum damage mechanics, which was originally proposed by Kachanov (1958), has been developed to the point that it can be effectively used in the design of practical engineering structures (Krajcinovic and Fonseka, 1981; Lemaitre, 1984, 1985). Some models have already been used in the petroleum industry, for example the damage model given by Valko and Economides (1993) in hydraulic fracturing treatments.

If only isotropic damage is considered, the damage theory can be characterized by a scalar damage variable D, which represents the concentration of microcracks and cavities existing in a cross-sectional area of an elementary volume with n orientations (Figure 1). If A is the total area and $\tilde{A}$ is the net cross-sectional area (Kachanov, 1958; Hult, 1975), then:

$$D = \frac{A - \tilde{A}}{A} \tag{3}$$

where $A - \tilde{A}$ is the damaged area in the cross-section.

Considering the cases of spheroidal pores or penny-shaped cracks embedded in a uniaxial tensile stress field, the relationship between the damage, D, and the crack density, χ, may be expressed as (Hult, 1987):

$$D \approx m\chi \tag{4}$$

where m is a parameter related to the crack geometry and the loading conditions.

In fact, damage mechanics provides a measure of material degradation which is only at the micro-mechanics scale. However, by using effective stresses and properties, the detailed information about fracture size, distribution and density is no longer important and, therefore, the material can be treated as a continuum medium. Furthermore, the damage variables can be measured experimentally using conventional standard testing methods (Chow and Wang, 1987a&b). For example, an effective net stress $\tilde{\sigma}$ acting on the net area $\tilde{A}$ can be expressed as:

$$\tilde{\sigma} = \frac{\sigma}{1 - D} \tag{5}$$

An attempt was made in this paper to develop an experimental technique to determine the compressibility of fractured rock.

THEORETICAL BACKGROUND

Damage Theory

Based on the concepts of continuum damage mechanics, any strain constitutive equation for a damaged material ($D \neq 0$) is derived from the same potentials as for a virgin material ($D = 0$) except that all the stress variables are replaced by effective stresses (Lemaitre, 1987). If the principal coordinate system is considered, the damaged stress-strain relation can be written in the form (Chow and Lu, 1991):

$$\{\epsilon\} = [\tilde{S}_{ij}]\{\sigma\} \tag{6}$$

where

$$\{\epsilon\} = \{\epsilon_1 \quad \epsilon_2 \quad \epsilon_3\}^T, \quad \{\sigma\} = \{\sigma_1 \quad \sigma_2 \quad \sigma_3\}^T \tag{7}$$

are principal strain and principal stress vectors, respectively.

The damaged compliance matrix $[\tilde{S}_{ij}]$ in equation (6) was also given by Chow and Lu (1991) as:

$$[\tilde{S}_{ij}] = \begin{bmatrix} \frac{1}{\tilde{E}_1} & -\frac{\tilde{\nu}_{21}}{\tilde{E}_2} & -\frac{\tilde{\nu}_{31}}{\tilde{E}_3} \\ -\frac{\tilde{\nu}_{12}}{\tilde{E}_1} & \frac{1}{\tilde{E}_2} & -\frac{\tilde{\nu}_{32}}{\tilde{E}_3} \\ -\frac{\tilde{\nu}_{13}}{\tilde{E}_1} & -\frac{\tilde{\nu}_{23}}{\tilde{E}_2} & \frac{1}{\tilde{E}_3} \end{bmatrix} \tag{8}$$

where

$$\begin{aligned} &\tilde{E}_1 = E(1-D_1)^2, \quad \tilde{E}_2 = E(1-D_2)^2, \quad \tilde{E}_3 = E(1-D_3)^2, \\ &\tilde{\nu}_{12} = \nu\frac{1-D_1}{1-D_2}, \quad \tilde{\nu}_{21} = \nu\frac{1-D_2}{1-D_1}, \quad \tilde{\nu}_{31} = \nu\frac{1-D_3}{1-D_1}, \\ &\tilde{\nu}_{13} = \nu\frac{1-D_1}{1-D_3}, \quad \tilde{\nu}_{23} = \nu\frac{1-D_2}{1-D_3}, \quad \tilde{\nu}_{32} = \nu\frac{1-D_3}{1-D_2}, \end{aligned}$$

D_1, D_2 and D_3 are the damage variables at their respective principal axes. It is worth mentioning that once damaged, the virgin isotropic material will generally behave like an anisotropic material. However, if $D_1 = D_2 = D_3 = D$, it is a case of isotropic damage.

Compressibility

By definition, the intrinsic compressibility is given by:

$$\beta = \frac{3(1-2\nu)}{E}. \tag{9}$$

Walsh(1965a) showed that the effective elastic constants are identical with those of a solid isotropic elastic body. In this case, one may write that:

$$\tilde{\beta} = \frac{3(1-2\tilde{\nu})}{\tilde{E}} \tag{10}$$

where $\tilde{\beta}$ is the effective compressibility.

EXPERIMENTAL PROCEDURE

Rock Specimen Preparation

Two rocks were used in this study, Berea sandstone and Cordoba Cream limestone. The standard cylindrical specimens, with diameter of 2.125" and length of 4.25", were prepared via coring in three different directions. The ends of the specimens were ground flat with a 80 grit aluminum oxide wheel. For Berea sandstone samples, one drilling direction was normal to the bedding planes. The samples were heated at 150°F in a oven for 24 hours and then air-cooled before testing, in order to minimize any possible moisture effects.

Polyolefin tubes were used to jacket both the rock sample and the end platens. The axial strain extensometer (MTS model 632.90B-04) and the circumferential extensometer (MTS model 632.92B-05) were mounted directly on the sample to measure both vertical and circumferential strains. The effect of the coating was investigated by using a standard aluminum sample.

Testing Facility

A servo-controlled MTS (Model 315) frame with an integral MTS 138 MPa (20,000 psi) built-in pressure vessel was used. The tests were performed under stroke control. A special computer programme was edited for the purpose of cyclic loading. The experimental set-up for P- and S-waves is shown in Figure 2. The detailed information was given by Scott et al. (1993). Two 486 IBM-PC's were used for the data storage: one is for the environmental parameters and another for the acoustic waveforms. The computer for the acoustic waveforms was also used to control the HP switch box via a GPIB interface. A Kipp & Zonen X-Y-Y(T) plotter was also used to plot the curves of load versus displacements in real time.

Test Procedures

The tests were carried out under mixed conditions of uniaxial cyclic loading and hydrostatic confining pressure (Figure 3). The purpose of uniaxial cyclic loading was to determine the materials properties and damaged tensor D; while the use of the hydrostatic confining pressure was to obtain compressibility values. The first cycle was used to determine the rock elastic properties, such as Young's modulus and Poisson's ratio and the first hydrostatic pressure was applied to determine the rock compressibility. After then, several loading-unloading cycles were applied to determine the effective modulus, Poisson's ratio and the damage tensor D.

The compressibility and fracture porosity may be obtained from the slope of volumetric strain versus pressure curve, as shown in Figure 4.

RESULTS AND DISCUSSION

Initial Porosity

The initial fracture porosity of rock can be determined by compressibility tests in which sufficiently high hydrostatic pressure is able to close all the pre-existing cracks; so that the total change in

porosity is equal to initial porosity (refer to figure 4). Similar procedures may be applied to measure the fracture porosity as we can also see from the same figure.

It is worth mentioning that, even when the applied pressure is sufficient to close all cracks, the modulus may still not be equal to that of the solid material, since frictional sliding at crack faces can occur (Walsh, 1965b). The highest values of hydrostatic pressures used in this study were 10,000 psi for Berea sandstone and 3,000 psi for Cordoba Cream limestone, as higher hydrostatic pressure may cause pore collapse (one specimen of Cordoba Cream limestone failed under the pressure of 5,000 psi). According to experimental data collected by Brace (1965), the compressibility of quartzitic sandstone under pressure of 500 bar is about 15% higher than that obtained in unjacketed specimens; while for Oak Hall limestone, only slight changes were found in the compressibility when the pressures were increased from 0 to 5,000 bars. The experimental results show that, even though low pressures were applied, the compressibility for the different damage levels only slightly changed at the highest applied pressures, indicating that the values of the fracture porosity measured at the applied pressure regions were sufficiently accurate for engineering purpose.

Poisson's Ratio

The effective Poisson's ratio was defined as the negative rate of change of lateral strain with axial strain at any particular stress (Walsh, 1965a); i.e.,

$$\tilde{\nu} = -\frac{d\epsilon_{\perp}}{d\epsilon_{\parallel}} \tag{11}$$

However, the measured values of both the radial strain and rate of change of the radial strain are larger than those of axial strain when the cracks are well-developed, demonstrating a significant effect of crack opening displacements. In order to simplify the problem, the model for a two-dimensional solid containing cracks is employed, which leads to:

$$\frac{\tilde{E}}{E} = \frac{\tilde{\nu}}{\nu} \tag{12}$$

Damage Tensor D

Before calculating the compressibility of fractured rock, one should determine the damage tensor D. In an uniaxial test, this tensorial parameter is assumed as axially symmetric and isotropic; i.e.

$$[D_{ij}] = \begin{bmatrix} D_1 & 0 & 0 \\ 0 & D_2 & 0 \\ 0 & 0 & D_2 \end{bmatrix} \tag{13}$$

According to equation (6), the elastic characteristics of the damaged material in uniaxial compression tests can be calculated by (Chow and Wang, 1987):

$$\tilde{E} = E(1 - D_1)^2 \tag{14}$$

and

$$\tilde{\nu} = \nu \frac{1 - D_1}{1 - D_2} \tag{15}$$

So, the damaged parameters can be written as:

$$D_1 = 1 - \sqrt{\frac{\tilde{E}}{E}} \tag{16}$$

and

$$D_2 = 1 - \frac{\nu}{\tilde{\nu}}\sqrt{\frac{\tilde{E}}{E}} \tag{17}$$

Using equation (12) yields:

$$D_2 = 1 - \sqrt{\frac{E}{\tilde{E}}} \tag{18}$$

As rocks are generally porous, the undamaged material properties can only be evaluated using the measured material properties. Combining equations (9) and (10) leads to:

$$\frac{\tilde{\beta}}{\beta} = \frac{E}{\tilde{E}}\frac{1-2\tilde{\nu}}{1-2\nu} \tag{19}$$

For isotropic material, $D_1 = D_2 = D_0$. This simplification results in a simpler expression for equation (15):

$$\tilde{\nu} = \nu. \tag{20}$$

Thus,

$$\frac{\tilde{\beta}}{\beta} = \frac{1}{(1-D_0)^2}. \tag{21}$$

The compressibility for a porous material was given by Walsh (1965a) and Brace (1965) as:

$$\frac{\tilde{\beta}}{\beta} = 1 + a\phi_p \tag{22}$$

where a is a constant equal to about 3 and ϕ_p is the pore porosity, the difference between total porosity and fracture porosity. So,

$$D_0 = 1 - \sqrt{\frac{1}{1+a\phi_p}}. \tag{23}$$

The fracture porosity may be determined from curves of pressure versus volumetric strain, as mentioned in the previous section. The values of D_1, E and ν were listed in Table 1.

Seismic Velocities

The dynamic properties may be obtained by P- and S-wave velocities. The following equations were used to calculate Young's modulus and Poisson's ratio (Jaeger and Cook, 1979):

$$E = \rho V_s^2\left(3 - \frac{V_s^2}{V_p^2 - V_s^2}\right) \tag{24}$$

and,

$$\nu = \frac{1}{2}\left(1 - \frac{V_s^2}{V_p^2 - V_s^2}\right) \tag{25}$$

where V_p and V_s are P- and S-wave velocities, respectively.

Table 1 also lists the values of dynamic Young's moduli and Poisson's ratios for every loading-unloading cycle of each specimen.

Measurements of Compressibility

The measured compressibility for all three Berea sandstone samples are tabulated in Table 2 and a sample is shown in Figures 5 and 6, for static and dynamic measurements, respectively. Generally speaking, the compressibility tends to increase with increasing damage and the initial change in compressibility with hydrostatic pressure are related quantitatively to the degrees of the damage. This is equally true for the results of limestone (Table 3). It is also found that the compressibility measured at higher hydrostatic confining pressures, are almost unchanged regardless of the difference in the damage, indicating that the fracture closing may only relate to the pressure.

Theoretically, the relationship between the ratio of original and effective compressibility and damage variable can be obtained by substituting (12) and (14) into (19):

$$\frac{\tilde{\beta}}{\beta} = \frac{1 - 2\nu(1 - D_1)^2}{(1 - 2\nu)(1 - D_1)^2} \tag{26}$$

A comparison study of theoretical results and experimental data is shown in Figure 7. The theoretical values agree well with the experimental data when the damage D_1 is large. If the damage is small, the values of calculated compressibility based on equation (26) are much lower that those obtained from experiments. Walsh (1965a) pointed out that sliding of crack surfaces past each other may take place after a crack has closed during the applied pressure. It is possible that the existing discrepancy for the small damage is due to the fact that the events of crack surface sliding are not as often as in the cases of high damage. Another possible reason is that as the failures of all samples are mostly along the axial loading direction, the crack interactions can be treated as pore-pore based. If that happens, there are more unbroken pores for the material with a low damage than the same material with a high damage. Consequently, a higher pressure is needed to close the pores.

The influence of the damage on the ratio of effective and original compressibility is drawn in Figure 8. One may find that these ratios are increased when the damage increases. Poisson's ratio has also a significant impact on the ratio of compressibility: the larger the Poisson's ratio, the larger the compressibility ratio.

CONCLUSIONS

Probably the more distinctive aspect regarding the application of continuum damage mechanics over the classic fracture mechanics is that the degree of damage can be measured in the laboratory. A technique is developed in this paper to measure the compressibility of fractured rock. The standard samples for uniaxial compression tests were tested in loading-unloading cycles with some

intervals of hydrostatic confining pressures. The purpose of cyclic loading was to create and develop the damage; while the confining pressure tests were to measure the compressibility. Two rocks were involved in this study: Berea sandstone and Cordoba Cream limestone.

The measured values of compressibility were then compared with the theoretical results: a large discrepancy existed when the damage was small. This is due to the fact that crack surface sliding for small damage does not occur as often as in the cases of large damage. Another possible reason is that the failures of all samples are mostly along the axial loading direction, the crack interactions are actually pore-pore based. In other words, there are more unbroken pores in the body of a material when the damage is small, and higher pressure is needed to close the pores than the cracks.

Poisson's ratio also has significant influence on the compressibility. In general, the higher values the Poisson's ratio, the larger magnitudes the compressibility.

Several areas, however, deserve further study. For one thing, it would be useful to know more about the acoustic properties of rocks. Preliminary results given in this study show that the compressibility obtained from the data of P- and S-wave are less sensitive. More important, from practical point of view, this technique can be readily used for underground geological engineering projects.

REFERENCES

Brace, W.F.: "Some new measurements of linear compressibility of rocks," Journal of Geophysical Research, 70, 391-398 (1965)

Bruner, W.M.: "Comment on 'Seismic velocities in dry and saturated cracked solids' by Richard J. O'Connell and Bernard Budiansky," Journal of Geophysical Research, 81, 2573-2576 (1976).

Chow, C.L. and Wang, J.: "An anisotropic theory of continuum damage mechanics for ductile fracture," Engineering Fracture Mechanics, 27, 547-558 (1987a).

Chow, C.L. and Wang, J.: "An anisotropic theory of elasticity for continuum damage mechanics," Engineering Fracture Mechanics, 33, 3-16 (1987b).

Chow, C.L. and Lu, T.J.: "A continuum damage mechanics approach to crack tip shielding in brittle solids," International Journal of Fracture, 50, 79-114 (1991).

Griffith, A.A.: "The phenomena of rupture and flow in solids", Proc. Trans. Royal Soc. A221, 163-198 (1920).

Hult, J.: "Damage-induced tensile instability," Trans. 3rd SMIRT, London, Paper L 4/8 (1975).

Hult, J.: "Introduction and general overview", Continuum Damage Mechanics: Theory and applications, CISM Courses and lectures No. 295, International Center for Mechanical Sciences, edited by D. Krajcinovic and J. Lemaitre, 1-36 (1987).

Irwin, G.R.: "Analysis of stresses and strains near the end of a crack traversing a plate", J. Appl. Mechanics, 24, 361-364 (1957).

Jaeger, J.C. and Cook, N.G.W.: "Fundamentals of Rock Mechanics," Third Edition, Chapman and Hall (1979).

Janson, J.: "Damage model of crack growth and instability," Engineering Fracture Mechanics, 10, 795-806 (1978).

Kachanov, L.M.: "On the creep fracture time," Izv. Akad. Nauk SSSR, Mekhan. Tverd. Tela, 8, 26-31 (1958).

Krajcinovic, D. and Fonseka, G.U.: "The continuous damage theory of brittle materials," J. appl. Mech., 48, 809-824 (1981).

Lemaitre, J.: "Formulation and identification of damage kinetic constitutive equations," Continuum Damage Mechanics: Theory and applications, CISM Courses and lectures No. 295, International Center for Mechanical Sciences, edited by D. Krajcinovic and J. Lemaitre, 37-89 (1987).

Lemaitre, J.: "How to use damage mechanics," Nucl. Engng Design 80, 233-245 (1984).

Lemaitre, J.: "A continuous damage mechanics model for ductile fracture," J. Engng Mater. Technol., 107, 83-89 (1985).

O'Connell, R.J. and Budiansky, B.: "Seismic velocities in dry and saturated cracked solids," Journal of Geophysical Research, 79, 5412-5426 (1974).

Salganik, R.L.: "Mechanics of bodies with many cracks," Izv. Akad. Nauk SSSR, Mekhan. Tverd. Tela, 135-143 (1973)

Salganik, R.L.: "Transport processes in bodies with a large number of cracks," Izv. Akad. Nauk SSSR, Mekhan. Tverd. Tela, 1534-1538 (1974).

Scott, T.E, Ma, Q., and Roegiers, J.-C.: "Acoustic velocity anisotropy induced during triaxial compression of Berea sandstone," Proceedings of 34th United States Symposium on Rock Mechanics, (in press).

Valko, P. and Economides, M.J.: "A Continuum-damage-mechanics model of hydraulic fracturing," JPT, 198-205 (March, 1993).

Vavakin, A.S. and Salganik, R.L.: "Effective characteristics of nonhomegeneous media with isolated nonhomogeneities," Izv. Akad. Nauk SSSR, Mekhan. Tverd. Tela, 58-66 (1975).

Walsh, J.B.: "The effect of cracks on the compressibility of rock," Journal of Geophysical Research, 70, 381-389 (1965a).

Walsh, J.B.: "The effect of cracks in rock on Poisson's ratio," Journal of Geophysical Research, 70, 391-398 (1965b).

Walsh, J.B.: "The effect of cracks on the uniaxial elastic compression of rocks," Journal of Geophysical Research, 70, 399-411 (1965c).

Walsh, J.B.: "The effect of cracks in rock on Poisson's ratio," Journal of Geophysical Research, 70, 5249-5257 (1965d).

Walsh, J.B., Brace, W.F., and England, A.W.: "Effect of porosity on compressibility of glass," J. Ame. Cera. Soci, 48, 605-608 (1965).

Table 1 The properties of fractured rock

cycle	static			dynamic		
	E Mpsi	v	D1	E Mpsi	v	D1
Berea sandstone (BSX2)						
0	3.29	0.37	0.00	3.43	0.37	0.00
1	2.53	0.29	0.12	2.64	0.29	0.12
2	2.63	0.30	0.11	2.71	0.30	0.11
3	2.75	0.31	0.09	2.64	0.30	0.12
4	2.56	0.29	0.12	2.68	0.28	0.12
5	2.14	0.24	0.19	2.60	0.28	0.13
6	2.61	0.29	0.11	2.68	0.28	0.12
Berea sandstone (BSY1)						
0	3.71	0.39	0.00	4.64	0.17	0.00
1	2.85	0.30	0.12	3.57	0.13	0.12
2	2.34	0.25	0.21	2.94	-0.35	0.21
3	2.36	0.25	0.20	2.94	-0.36	0.21
4	2.20	0.23	0.23	3.16	-0.34	0.18
5	2.02	0.21	0.26	3.61	-0.12	0.12
Berea sandstone (BSZ2)						
0	3.75	0.39	0.00	4.34	0.21	0.00
1	2.88	0.30	0.12	3.34	0.16	0.13
2	1.81	0.19	0.31	3.20	0.17	0.14
3	2.45	0.25	0.19	3.15	0.19	0.15
Cordoba Cream limestone (LMX1)						
0	4.41	0.16	0.00			
1	1.84	0.06	0.35			
2	3.78	0.14	0.07			
3	3.11	0.11	0.16			
Cordoba Cream limestone (LMY2)						
0	4.92	0.16	0.00			
1	4.22	0.14	0.07			
2	2.56	0.08	0.30			
3	3.23	0.11	0.19			
4	2.40	0.08	0.30			
5	2.91	0.09	0.23			
6	2.21	0.07	0.33			
7	2.18	0.07	0.33			
Cordoba Cream limestone (LMZ1)						
0	4.20	0.20	0.00			
1	3.61	0.17	0.07			
2	1.8	0.09	0.35			
3	1.92	0.09	0.32			
4	2.03	0.10	0.30			
5	2.07	0.10	0.30			
6	2.02	0.10	0.31			
7	2.02	0.10	0.31			

Table 2 Compressibility of Berea sandstone

sample	Hydrostatic confining pressure (psi)							
No.	2000	3000	4000	5000	6000	7000	8000	9000
BSX2	1.75	1.34	1.13	0.98	0.89	0.80	0.76	0.78
	1.33	1.01	0.87	0.79	0.74	0.68	0.67	0.70
	1.55	1.07	0.89	0.81	0.74	0.69	0.66	0.70
	1.76	1.14	0.94	0.83	0.76	0.71	0.69	0.70
	2.18	1.35	1.06	0.92	0.82	0.76	0.73	0.75
	2.50	1.53	1.19	0.99	0.87	0.81	0.76	0.76
BSY1	4.0	1.28	1.09	0.99	0.93	0.90	0.89	0.86
	3.15	1.74	1.22	1.08	0.99	0.95	0.94	0.95
	5.32	1.76	1.15	1.03	0.96	0.91	0.91	0.93
BSZ2	1.79	1.41	1.09	0.99	0.89	0.82	0.73	0.84
	1.20	0.95	0.82	0.77	0.71	0.71	0.68	0.67
	1.52	1.01	0.85	0.78	0.73	0.65	0.63	0.66
	2.32	1.46	1.14	0.97	0.85	0.80	0.77	0.75
	2.08	1.38	1.10	0.96	0.86	0.79	0.76	0.75

Table 3 Compressibility of Cordoba Cream limestone

sample	confining pressure (psi)		
No.	1000	2000	3000
LMX1	3.62	0.52	0.48
	3.57	0.47	0.45
	6.40	1.56	1.02
LMY2	1.72	0.51	0.59
	1.19	0.42	0.36
	1.99	0.44	0.40
	2.09	0.44	0.35
	3.40	0.53	0.37
	5.95	0.68	0.50
	6.29	0.66	0.44
LMZ1	1.60	1.00	1.00
	2.77	0.97	0.86
	3.13	1.04	0.95
	4.34	1.12	0.98
	5.88	1.23	1.05
	8.33	1.64	1.35
	9.98	2.00	1.67

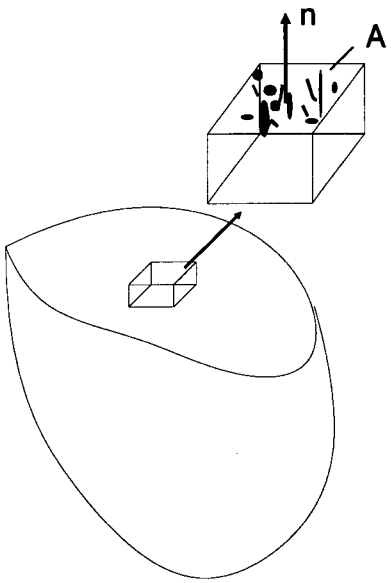

Figure 1. The dafinition of damage.

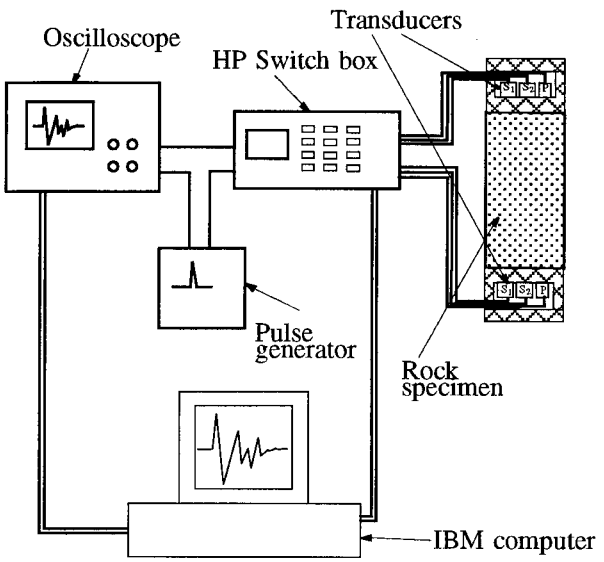

Figure 2. Experiment set-up for acoustic measurements of rocks.

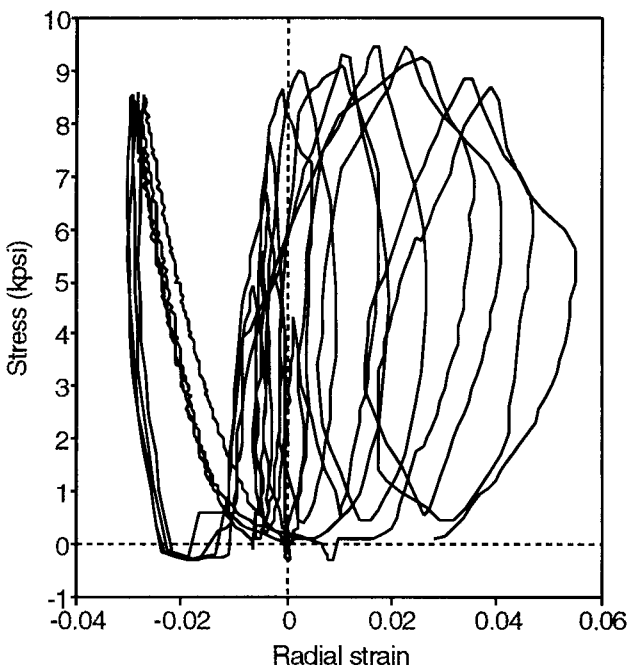

Figure 3. An example of stress-strain curve.

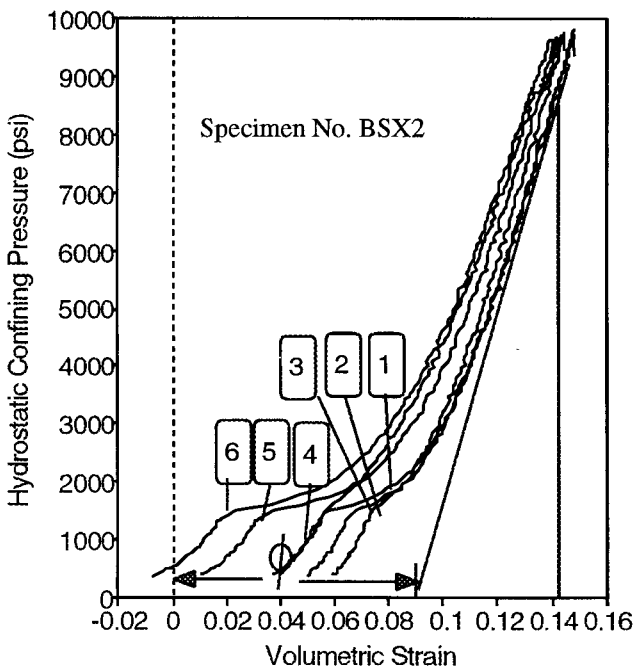

Figure 4. Hydrostatic confining pressure vs. volumetric strain.

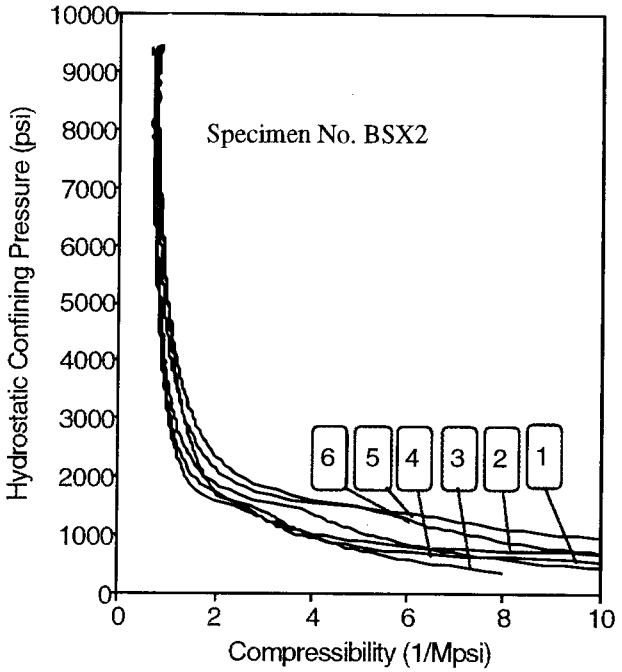

Figure 5. Static compressibility measurements.

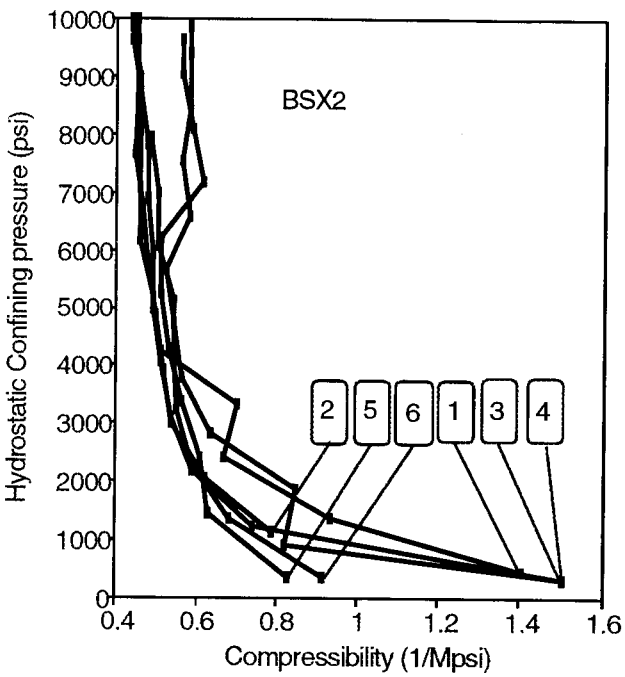

Figure 6. Dynamic compressibility measurements.

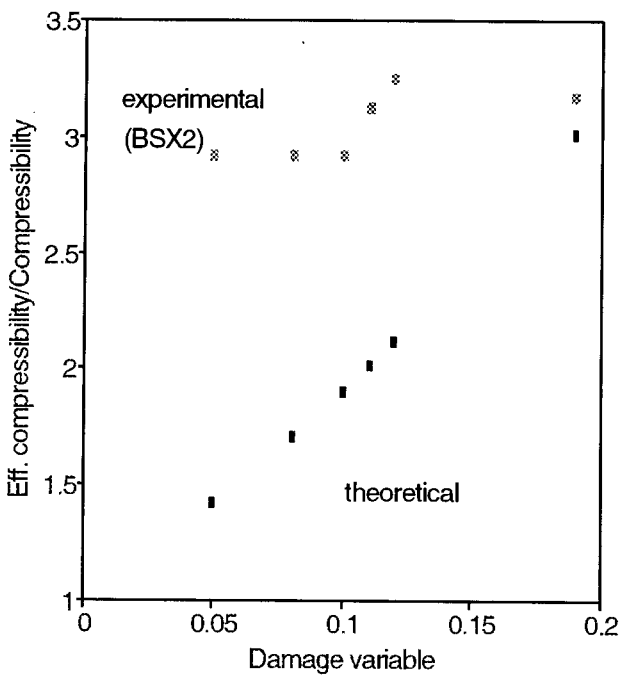

Figure 7. A comparison study of theoretical results and experimental data.

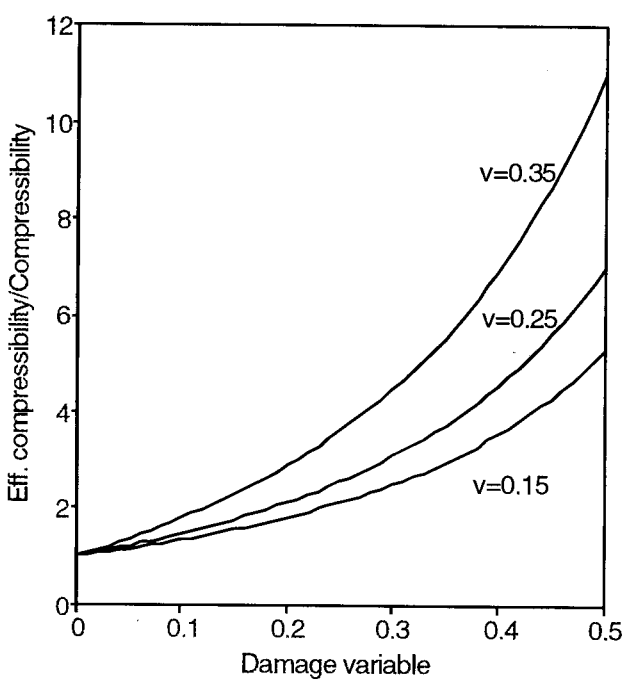

Figure 8. The influence of the damage on compressibility.